JOURNAL OF MORPHOLOGY 275:1145–1160 (2014)

Functional Anatomy and Kinematics of the Oral Jaw System During Terrestrial Feeding in *Periophthalmus barbarus*

Krijn B. Michel,[1]* Dominique Adriaens,[2] Peter Aerts,[1,3] Manuel Dierick,[4] and Sam Van Wassenbergh[1,2]

[1]*Department of Biology, Universiteit Antwerpen, Universiteitsplein 1, B-2610 Antwerpen, Belgium*
[2]*Department of Biology, Evolutionary Morphology of Vertebrates, Ghent University, K.L. Ledeganckstraat 35, B-9000 Gent, Belgium*
[3]*Department of Movement and Sports Sciences, Ghent University, Watersportlaan 2, B-9000 Gent, Belgium*
[4]*Department of Physics and Astronomy, Centre for X-ray Tomography (UGCT),Ghent University, Proeftuinstraat 86, 9000 Ghent, Belgium*

ABSTRACT The Atlantic mudskipper, *Periophthalmus barbarus*, is an amphibious fish that successfully overcomes the numerous physical challenges of capturing prey in a terrestrial environment. However, it is unclear what changes in the morphology and function of the feeding apparatus contribute to the mudskipper's successful transition from aquatic to terrestrial capture of prey. In particular, how does the mudskipper achieve effective prehension of land-based prey using its percomorph feeding apparatus? To address that question, we performed a morphological analysis of the feeding apparatus of *P. barbarus* based on microcomputed tomography scanning, histological sectioning, and dissections as well as a kinematic analysis based on high-speed video and X-ray video to quantify the movements of the oral jaw apparatus elements. Our results show that the neurocranium remains in a fixed position relative to the pectoral girdle as the fish pivots over its pectoral fins toward the prey. The premaxilla rotates dorsally and protrudes downward over the prey. The dentary is rotated ventrally over an angle of 120°, which is facilitated by an intramandibular joint. These motions of the neurocranium, premaxilla, and dentary reorient the mouth aperture so it is parallel to the substrate, thereby allowing the jaws to be placed over the prey. The prey is grabbed between the oral teeth or scooped into the mouth primarily via rapid closing motion of the lower jaw. This analysis of *P. barbarus* clarifies the morphological and kinematic characteristics required by fish to become successful terrestrial feeders at the environmental transition between water and land. J. Morphol. 275:1145–1160, 2014.

KEY WORDS: mudskipper; morphology; prey capture; Gobiidae

INTRODUCTION

The shift from an aquatic to a terrestrial environment is among the most important transitions in vertebrate evolutionary history (Sayer and Davenport, 1991; Daeschler et al., 2006). A well known example is the fish-tetrapod evolutionary transition during the late Devonian. The identification of the morphological and physiological changes required to make this transition and how these modifications to the vertebrate body evolved are subjects of much debate in evolutionary biology, comparative anatomy, and paleontology (e.g., Boisvert, 2005; Shubin et al., 2006; Downs et al., 2008; Ahlberg et al., 2008; Pierce et al., 2013).

However, this historic example is not the only occurrence of a water-to-land transition within the vertebrates. Water-to-land transitions have occurred independently in several vertebrate lineages within this group. For example, the acquisition of an amphibious or terrestrial lifestyle has occurred multiple times within actinopterygian fishes, such as in blennies (Blenniioidei; Nieder, 2001; Hsieh, 2010) and mudskippers (Oxurcinae; Stebbins and Kalk, 1961; Sponder and Lauder, 1981). Most previous studies of these taxa have only addressed modifications in behavior and physiology, but studying the morphological and biomechanical changes that occurred in response to the aquatic-terrestrial niche shift within extant groups may help us to understand the functional challenges and evolutionary changes in morphology during the fish to tetrapod transition (Ashley-Ross et al., 2013).

Contract grant sponsor: New Research Initiative Grant from the Special Research Fund (NOI-BOF) of the University of Antwerp (to S.V.W. and P.A).

*Correspondence to: Krijn Michel, Universiteit Antwerpen, Department of Biology, Laboratory for Functional Morphology, Universiteitsplein 1, B-2610 Antwerpen, Belgium. E-mail: krijn.michel@uantwerpen.be

Received 30 August 2013; Revised 3 April 2013;
Accepted 4 April 2014.

Published online 5 May 2014 in
Wiley Online Library (wileyonlinelibrary.com).
DOI 10.1002/jmor.20291

The physical conditions of the terrestrial realm pose several challenges to ancestral aquatic organisms. These challenges apply to the evolution of a musculoskeletal system that is suited for over-land movement, but they are also associated with the capture and transport of food on land (Ashley-Ross et al., 2013). Among the amphibious fish species that are capable of performing terrestrial excursions, only a fraction have been found to be proficient in the capture of terrestrial prey (e.g., Gordon et al., 1969; Gillis, 1998; Schoenfuss and Blob, 2003; Hsieh, 2010; Gibb et al., 2011; Van Wassenbergh, 2013). The lack of terrestrial feeders suggests that additional physical constraints apply to the evolution of terrestrial feeding, next to gaining the capacity to excess the terrestrial environment. The following physical constraints apply in a terrestrial environment. First, the effect of gravity is experienced to a greater extent compared with an aquatic environment because air provides negligible buoyancy. The lack of buoyancy imposes a serious constraint on the terrestrial mobility of vertebrates that are adapted primarily for movement in water, which also limits their terrestrial foraging performance (Van Wassenbergh et al., 2006; Herrel et al., 2012; Van Wassenbergh, 2013). Second, suction feeding is the most common feeding mechanism used in aquatic environments (e.g., Liem, 1990; Summers et al., 1998), but it does not function in the terrestrial environment because air is 900 times less dense and 80 times less viscous than water (Lauder, 1985; Herrel et al., 2012). Consequently, air flows are unsuitable for the transport of most prey. Third, the physical properties of air restrict the major terrestrial prey types that are accessible to novel terrestrial feeders; prey is restricted to lay or crawl on the substrate rather than float or swim in the water column. Animals that feed in a terrestrial environment must have adapted to overcome all of these challenges, to successfully capture prey from the substrate (Herrel et al., 2012).

A combination of behavioral and morphological adaptations are required to position of the jaws of fishes to achieve effective prehension of prey on land. The eel catfish (*Chanallabes apus*) has been found to feed on terrestrial insects after propelling itself out of the water, where it uses a downward inclination of the head (up to 70°) to place its jaws over the prey (Van Wassenbergh et al., 2006; Van Wassenbergh, 2013). The downward inclination of the head requires substantial intervertebral flexion of the eel-like body, while providing support with a portion of the body to maintain a coordinated positioning of the head (Van Wassenbergh, 2013). However, alternative adaptations may be required as not all terrestrial feeding fishes have the required intervertebral bending or eel-like body, for example, blennies and mudskippers (Nowroozi and Brainerd, 2013). A logical solution to this problem would be a subterminal oriented mouth, which is found in some specialized groups of benthic aquatic feeders (e.g., biting coral reef fishes, loricariid, and mochokid catfishes; Konow et al., 2008; Geerinckx et al., 2011; Konow and Bellwood, 2011). However, most blennies and mudskippers have a terminal mouth aperture (Gregory, 1933; Burgess et al., 1990).

Mudskippers are known to readily locomote and forage on the intertidal mud flats of estuarine mangrove swamps, while supporting themselves on their pectoral and pelvic fins (Harris, 1960; Sponder and Lauder, 1981). A previous study found that the mudskipper species *Periophthalmus barbarus* can reorient its jaws by pivoting forward on its pectoral fins (Sponder and Lauder, 1981). However, this pivoting only causes a ventral rotation of the head of about 20°, which is insufficient to orient the open mouth plane parallel to the substrate and bring the mouth downward over the prey. Consequently, additional and as of yet unquantified movements of the skull, pectoral girdle, and upper and lower jaws might be involved in positioning the gape.

The main goal of our study is to identify the functional attributes of the cranial system that allow Atlantic mudskippers (*P. barbarus*) to capture ground-based prey on land. In particular, how is *P. barbarus* morphologically equipped to position its gape above its prey, before scooping or grabbing it between its jaws? First, the functionality of the oral jaw system cannot be understood fully without a clear understanding of the morphology of the cranial musculoskeletal system, therefore we provide a morphological description of the structures involved. Second, we provide a quantitative assessment of the oral jaw movements that occur during prey capture. These analyses provide a better understanding of how mudskippers capture terrestrial prey.

MATERIALS AND METHODS

Study Animals

Four wild-caught adult Atlantic mudskippers (9.9 ± 1.8 cm standard length), *P. barbarus* (Linnaeus, 1766), were obtained commercially. Two additional adult individuals were sacrificed using an overdose of MS-222 (Sigma Chemical) and one was used for computed tomography (CT) scanning, whereas the other was prepared for histological sectioning (see later). The four live animals were housed in individual plexiglas aquaria ($35 \times 18 \times 30$ cm) during testing and recording. The aquaria were equipped with a plexiglas ramp and a terrestrial excursion area with a transparent floor and sides. A constant temperature of 27°C was maintained, with a 12:12 h light:dark cycle. All of the specimens used in this study were handled according to University of Antwerp Animal Care protocols.

CT-Scans

A *P. barbarus* specimen with a total length of 6.9 cm was scanned using the modular micro-CT setup at Ghent University (Masschaele et al., 2007). The setup was a dual-head X-ray tube with a transmission-type head, with a focal spot size of 900 nm at a tube voltage of <40 kV for high resolution. In total, 822 projections of 570×608 pixels were recorded, which

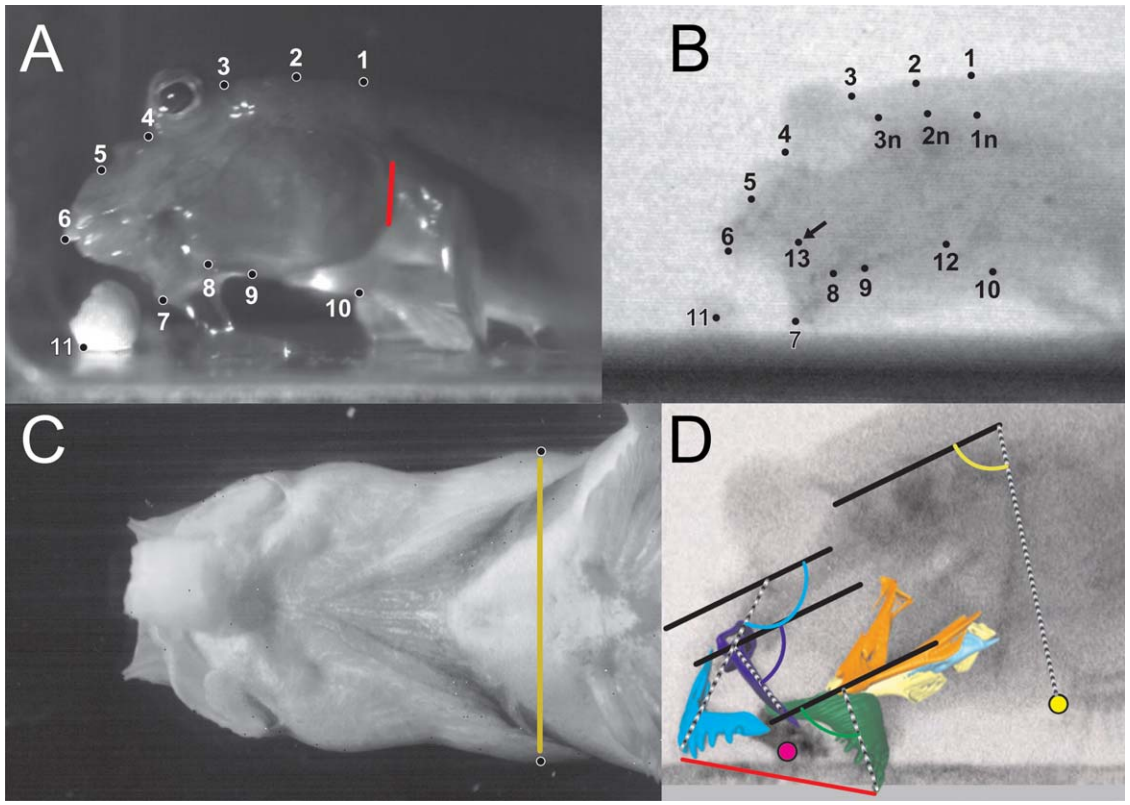

Fig. 1. *P. barbarus*, illustration of the position of the landmarks on the head of a mudskipper and their representative structures. (**A**) Landmarks that were followed during prey capture on the external high-speed videos (Points 1 to 11). The red line indicates the position of the opercular opening. (**B**) Landmarks traced on the high-speed X-ray videos (Points 1 to 13) were mostly identical with those of the external high-speed video. The 1n to 3n points allowed us to verify the alignment of number 1 to 3 with the roof of the neurocranium. The arrow indicates the landmark for the posterior end of the maxilla. (**C**) Landmarks followed in ventral view on external high-speed recording. The points at the end of yellow line show where the opercular expansion was measured. (**D**) Illustration of the angles measured relative to the neurocranium (black line) for each marked structure (Color of each structure matches with the graph color, see Fig. 8).

covered the whole head and part of the trunk. The raw data were processed and reconstructed using the in-house CT software Octopus (Vlassenbroeck et al., 2007) and rendered using Amira (Mercury Systems). The CT-rendered images were color coded to distinguish separate ossified units, where stiff and rigidly interconnected bones were given a single color.

Histological Sections

One specimen (standard length = 9.9 cm) was used to produce serial histological sections. The head was processed by decalcifying (using Decalc) and embedding in Technovit 7100 (Kulzer Heraus), before it was sectioned using a Leica Polycut microtome equipped with tungsten carbide-coated metal blades. The 5 μm sections were stained with toluidine, placed on glass slides, and sealed with ethyl acetate-coated cover slips. These sections were used to determine the precise attachment positions of the tendons and ligaments, and to identify the tissue types.

Kinematic Analysis

Simultaneous high-speed video recordings were captured from lateral and ventral views of *P. barbarus* feeding on land. *P. barbarus* were fed pieces of Brown shrimp or housefly grubs while recording using two Redlake cameras (1280 ×1024 pixels; Redlake, San Diego, CA): a Redlake MotionPro HS1000 and a MotionScope M3 at 500 frames per second. Several bright LEDs were used for illumination. The food items provided were approximately 7.5 mm in length (the grubs were 3 mm in diameter), which was approximately <80% of the maximal gape size of the fish. Each animal was recorded at least five times. Using these videos, two recordings were selected for further analysis per animal, based on the quality of the image sharpness and contrast of the recording.

In addition to the external video recordings, high-speed X-ray videos were obtained for each of the four individuals (Fig. 1). These recordings were produced according to the method described by Snelderwaard (2002) using a Philips Optimus M 200 X-ray generator (Royal Philips Electronics NV, Eindhoven, the Netherlands) coupled to a 14 inch image intensifier (6 inch zoom function) and a Redlake Motion Pro 2000 camera (1280 ×1024 pixels; Redlake, San Diego, CA) recording at 250 frames per second. To obtain marker-based information about bony element kinematics for two individuals, the animals were anesthetized using MS-222, and small radio-opaque metal makers were placed subcutaneously in close proximity to the lower jaw, premaxilla, hyoid, and skull roof using hypodermic needles. These procedures were not performed for the other individuals because the resolution and contrast of the recordings were sufficient. In recordings captured at a low frame rate, movements of some none-bony elements were delineated well enough to follow without radio-opaque metal markers.

The video recordings were digitized and analyzed to quantify the movement of the elements involved in prey capture by *P. barbarus*. The position of several anatomical landmarks, that is,

TABLE 1. Mechanical units and corresponding structures

Mechanical unit	Associated ossified structures
Neurocranium	mesethmoideum, lateroethmoideum, frontale, parasphenoideum, sphenoticum, pteroticum, epioticum, exoccipitale, vomer.
Pectoral girdle	cleithrum, scapula, coracoideum, supracleithrum, post-temporale.
Gill cover	operculare, suboperculare, 1st to 5th branchiostegal rays.
Suspensorium	quadratum, metapterygoideum, symplecticum, preoperculare, hyomandibulare, ectopterygoideum.
Hyoid apparatus	ceratohyale (anterior and posterior), hypohyale, interhyale, urohyale, basihyale
Upper jaw	praemaxillare, maxillare, palatinum, lacrymale.
Lower jaw	dentale, anguloarticulare, retroarticulare

The functional mechanical units of Periophthalmus barbarus during feeding as defined sensu Gans (1969) and associated morphological structures.

several points along the roof of the neurocranium (Fig. 1A Points 1–3), the rostral-most eye socket edge (Point 4), dorsal point of the upper jaw (Point 5), upper jaw tip (Point 6), the lower jaw tip (Point 7), a proximal point along the lower jaw (Point 8), a fixed point on the hyoid (Point 9), the ventral tip of the cleithrum (Point 10), and the position of the food item (Point 11), were tracked over time frame by frame in a lateral view using ImageJ software (NIH, Texas; Fig. 1A). Landmarks at the posterior edges of the opercula were tracked in the ventral view (Fig. 1C). The digitized *x*- and *y*-coordinates of the landmarks in ventral and lateral views were used in the kinematical analysis. The position of the neurocranium reflects the movement of the fish in the global frame of reference. Thus, by tracking the roof of the neurocranium immediately anterior to the first vertebra, the head pitch angle, and anteroposterior movements of the head were followed during feeding. The *x*- and *y*-coordinates of the anatomical landmarks were set relative to the frame of reference of the neurocranium, thereby subtracting the movement of the whole fish from each of the individual anatomical elements (Fig. 1D). The radiopaque markers in the high-speed X-ray recordings were digitized in a similar manner.

After manual digitization, the data noise was reduced by applying a fourth-order Butterworth zero phase-shift lowpass filter to the data, before velocities were calculated (cutoff frequency of 12 Hz; Winter, 2004; Erer, 2007). The data from the high-speed X-ray recordings were filtered in a similar manner. The timing of maximum gape was set as time zero.

The following kinematic variables were calculated based on the digitized points (Fig. 1A,B): lower jaw depression (angle from a proximal point on the dentary to the tip, $-\Delta y$ lower jaw tip), upper jaw elevation (angle of the base of the eye and upper jaw tip, Δy upper jaw tip), gape (distance between the upper and lower jaw tips), hyoid depression (angle of the base and point along the hyoid, $-\Delta y$ hyoid point), maxilla angle (angle of the anterior base of the maxilla and posterior maxilla tip, $-\Delta y$ maxilla), distance to food (distance between center of the gape and the food item), the opercular expansion (distance between the posterior opercular tips, Δy opercular tips), cleithrum depression (angle of the base neurocranium and ventral cleithrum tip, $-\Delta x$ cleithrum tip), and neurocranium pitch (angle of the neurocranium relative to the earth frame of reference, $-\Delta y$ neurocranium). The angles relative to the neurocranium axis were defined as positive (as shown in Fig. 1D, relative to the black neurocranium line). The X-ray recordings were subjected to the same kinematic analysis as the external video recordings.

An analysis of variance was used to test for differences in the kinematic variables between individuals. All reported standard deviation and standard error of the mean correspond to the variation between the individuals ($N = 4$).

By combining high-speed video recording, high-speed X-ray video recording, and CT-scan data, we were able to define functional morphological mechanical units as a group of one or more discernable elements that participate as a whole in complex movements (*sensu* Gans, 1969).

The identification and nomenclature of the skeletal, ligamentous, and muscular elements of the feeding apparatus in *P. barbarus* followed the morphological descriptions and examples given by Gregory (1933), Barel et al. (1976), Anker (1974, 1977, 1985), Elshoud-Oldenhave (1979), and Winterbottom (1973). The full scientific terminology of the osteology of the mudskipper in the figures was based on Harrington (1955) and Arratia (1987). The terminology within the text was based on data from the Zebrafish Model Organism Database, University of Oregon, Eugene, OR 97403-5274; URL: http://zfin.org/; 2013 (Bradford et al., 2011).

RESULTS

Morphology

We present our results on the morphology of the *Periophthalmus* feeding apparatus by defining separate mechanical units (*sensu* Gans, 1969). Seven mechanical units could be distinguished in the feeding apparatus of *P. barbarus*: neurocranium, pectoral girdle, gill cover, suspensorium, hyoid apparatus, upper jaw, and lower jaw (Table 1, Figs. 2, 3, 4, 5. and 6). To facilitate a better understanding of the oral jaw function during prey capture, we describe the skeletal elements of each mechanical unit and determined their functional connections such as muscles, ligaments, or other connective tissues.

Neurocranium. The neurocranium comprises several fused bones (Table 1) and serves as a supporting structure for other mechanical units. The neurocranium is reduced surrounding the orbit with only the frontal bone and parasphenoid connecting the vomer and ethmoid bones to the more posterior neurocranium (Figs. 2 and 3). The mesethmoid bones are reduced anteriorly and positioned between the lateroethmoid bones, while the frontal bone is fused to both mesethmoid and lateroethmoid bones (Figs. 2A, 4, and 5). The frontal bone is reduced to a single narrow arch between the orbit, widening just posterior of the orbit. Together, the parasphenoid, ethmoid, and frontal bones provide structural support to the upper jaw and they serve as points of attachment for the adductor arcus palatini and adductor mandibulae A1 muscles (Fig. 2B,C). Immediately anterior to the hyomandibular articulation with the neurocranium, the sphenotic extends in an anterolateral direction and acts as an insertion site for the levator arcus palatini and part of the dilator operculi muscles (Fig. 2C). The posterior surface of the neurocranium serves as the site of insertion for the opercular muscles, that is, the levator operculi and adductor operculi (Fig. 2B,C). The neurocranium connects rigidly to the vertebral column and

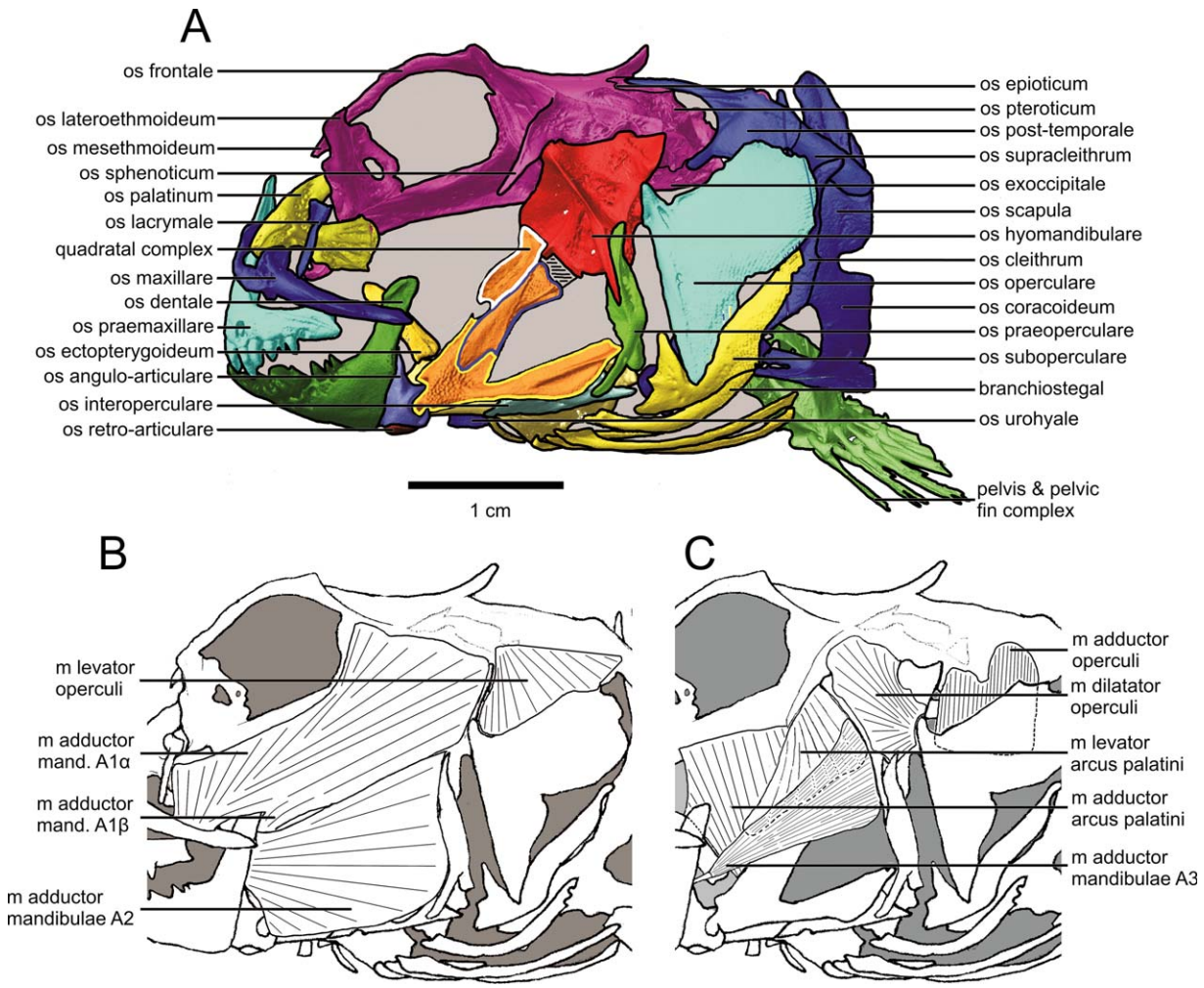

Fig. 2. (**A**) *P. barbarus*, overall skeletal body plan of in lateral view, without ligaments or muscles. Each color represents an ossified unit (os). The quadratal complex (orange) consists of the fused metapterygoid (white outline), symplectic (blue outline), and quadrate (yellow outline). (**B**) Excerpt of the lateral view showing the position of the adductor mandibulea A1α, A1β, A2, and levator operculi muscles (m). (**C**) Lateral view of the more medial muscles, such as adductor mandibulae A3, dilatator operculi, adductor operculi, levator arcus palatini, and adductor arcus palatini.

is connected to the cleithrum via the post-temporal and supracleithrum.

Pectoral girdle. In *Periophthalmus*, the cleithrum arches from the dorsolateral side of the head, immediately posterior of the opercula, toward the medioventral side, medial of the branchiostegal rays (Figs. 2A and 3). The cleithrum connects the cranium to the pectoral and pelvic fins. The supracleithrum rests between an ascending process of the cleithrum and the cleithrum itself, and the post-temporal connects the supracleithrum to the neurocranium. The post-temporal is V-shaped and has two connections with the neurocranium: a ventral connection with the exoccipital and a dorsal connection with the epiotic. Direct manipulation of the cleithrum during dissections of fresh material and inspection of X-ray recordings revealed little or no anteroposterior movement of the pectoral girdle.

Gill cover. The gill cover primarily comprises the subopercle and opercle, and is supported by the branchiostegal rays. The second, third, and fourth branchiostegal rays contribute mainly to the floor of the opercular cavity (Figs. 2 and 3). The opercular skin fold is fused almost completely to the body, leaving only a small opercular opening at the level of the hyomandibula (~1 cm wide in adults, the red line in Fig. 1A). As the morphology of the gill cover in *P. barbarus* is largely identical to that of most aquatic teleost species, we refer to the morphology of *Haplochromis elegans* for further description (Anker, 1985).

Suspensorium. The suspensorium is triangular in shape, where the quadratal complex, hyomandibula, and preopercle are connected to each other. In *Periophthalmus*, the quadratal complex comprises the symplectic, metapterygoid, and quadrate, and these elements are connected to

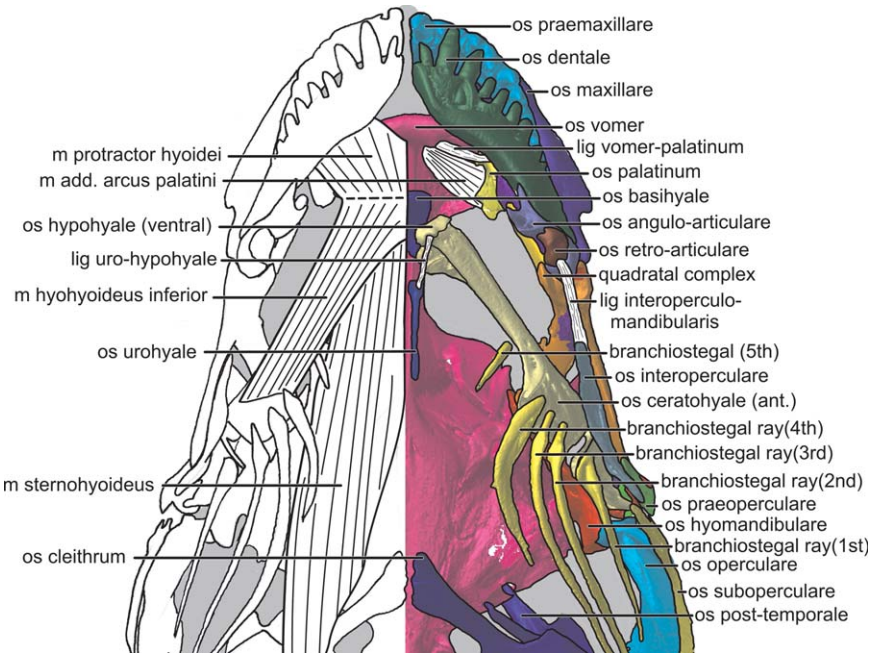

Fig. 3. *P. barbarus*, ventral view of the CT-reconstruction of head indicating the position of the main lower jaw adductors and ligamentous (lig) connections.

form a single rigid unit (Fig. 2A). The quadratal complex forms the anteroventral corner of the suspensorium with the metapterygoid and it connects posterodorsally with the hyomandibula (Fig. 2A). The posterior arm of the quadratal complex, which is part of the quadrate, is connected with the preopercle (Figs. 2A and 4). The preopercle forms the posteroventral corner of the triangular suspensorium and ascends in a dorsal direction to connect with the broad hyomandibula. Although the hyomandibula is not fused with the other elements of the suspensorium, it does not permit any obvious movement in the anteroposterior direction when manipulated during dissections. A broad synchondrotic connection is found between the hyomandibula and the symplectic (Fig. 2A). The hyomandibula articulates with the neurocranium through two saddle-shaped joints, that is, one anterior and one posterior on the mediodorsal side of the hyomandibula. These joints of the hyomandibula allow the suspensorium to rotate along the axis that connects these two joints. The ectopterygoid is suspended between the quadrate and the palatine by the quadrato-palatine ligament. This connection does not inhibit the medial-lateral movement of the suspensorium. The suspensorium and neurocranium are connected by the adductor arcus palatini muscle, which originates from the parasphenoid and inserts onto the medial side of the quadrate and metapterygoid. From the posteroventral side of the sphenotic, the levator arcus palatini muscle connects to the lateral side of the metapterygoid and quadrate (Fig. 2C). The quadrate bears the mandibular articulation facet on which the lower jaw rotates. The quadrate facet of this joint is broad and saddle-shaped, which constrains translation in the lateral-medial direction within the joint. The adductor mandibulae A3 muscle originates from the ventral part of the hyomandibula and has a tendinous insertion onto the anguloarticular bone (Figs. 2C and 6B). Similarly, the preopercle and the posterior arm of the quadrate form the insertion point for the adductor mandibulae A2 muscle, which is connected to the coronoid process of the dentary (Fig. 2B).

Hyoid. The hyoid arch has four main parts: the posterior ceratohyal, which is connected by a synchondrosis to the anterior ceratohyal, and the dorsal and ventral hypohyal, which are fused to the anterior ceratohyal. Together they form the main moveable unit of the hyoid, immediately posterior to the lower jaw. The hyoid articulates with the hyomandibula via the interhyal, which is positioned medial to the preopercle. The urohyal is connected ligamentously to the anterior hypohyal. The basihyal (glossohyal in Anker, 1977) is loosely connected as it arches dorsally over the anterior ceratohyal (Fig. 3). The protractor hyoidei muscle connects the hyoid to the dentary. The sternohyoideus muscle connects tendinously to the urohyal, where the tendons continue as ligaments to connect the urohyal to the hypohyals. The hyohyoideus inferior muscle connects posteriorly from the protractor hyoidei muscle.

Upper jaw. The most complex of the mechanical units in *P. barbarus* is the moveable upper jaw

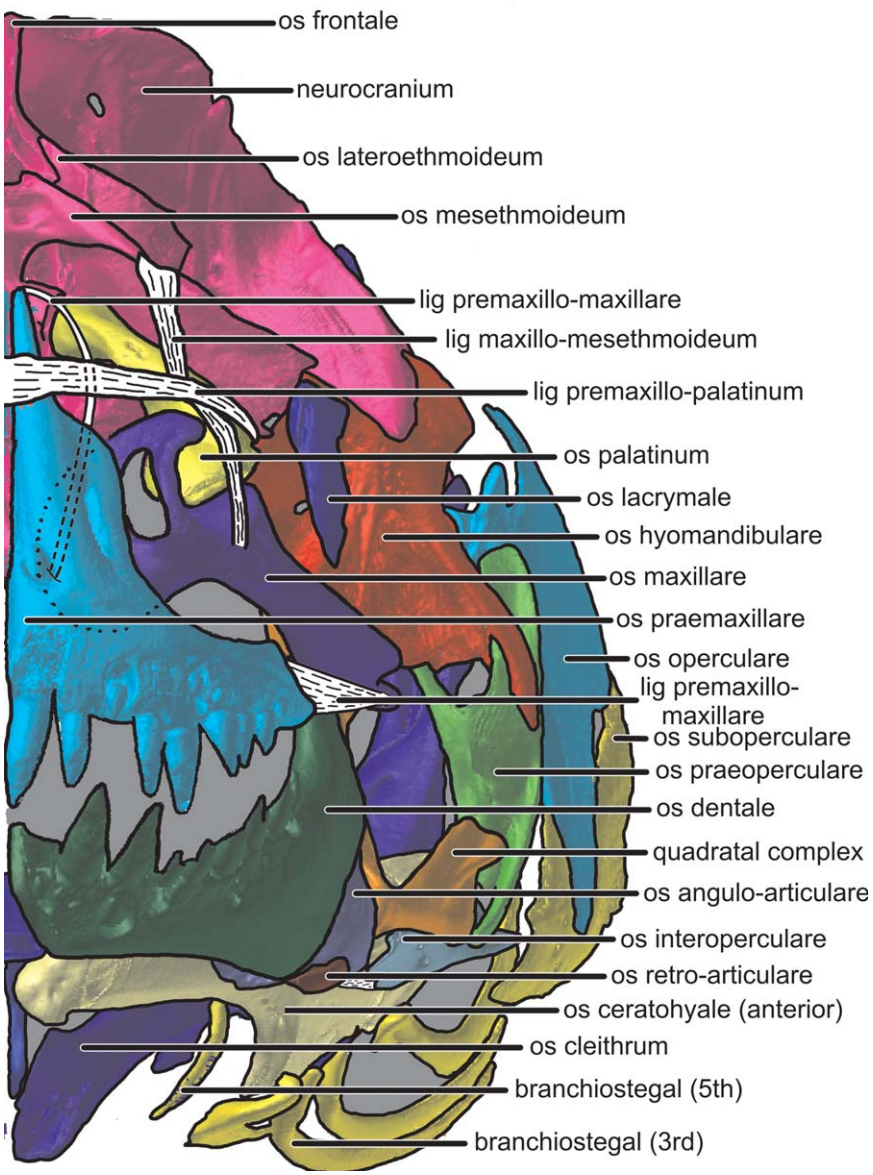

Fig. 4. *P. barbarus*, frontal view of the left side of the skull, including the ligaments involved in feeding. The premaxillo-maxillary ligament running behind the rostral cartilage is similar to the rostral cartilage ligament found in *G. aculeatus* (Anker, 1974). Pectoral fins are not shown.

apparatus, which mainly comprises the premaxillae, maxillae, and palatine bones. The skeletal elements of the upper jaw are interconnected only by ligaments and muscles, and none of the skeletal elements of the upper jaw are fused or rigidly connected to each other (Figs. 4 and 5). The palatine can be divided into two functionally different areas: an anterior part that forms an ascending arch and a posterior part that forms a plate, which broadens in the sagittal plane (Figs. 4 and 5 and Figs. 3 and 5, respectively). The anterior part of the palatine articulates with the neurocranium at its most dorsoposterior point via a joint with the lateral ethmoid bone and articulates anteroventrally with the maxilla (Figs. 4 and 5). The posterior portion of palatine is attached ligamentously and musculously to the vomer through the medial side of the palatal plate (Fig. 3). Overall, the palatine forms an articulating bridge between the maxilla and neurocranium, which is mediated by the vomeropalatine ligament, the quadratopalatine ligament, and an anterior slip of the adductor arcus palatini muscle (Figs. 3 and 5). The maxilla forms an elongated arch, which runs from the anterior palatine to the coronoid process of the dentary. The posterior end of the maxilla is flattened dorsoventrally, with connective tissue attaching it to the dentary on its dorsal side and a

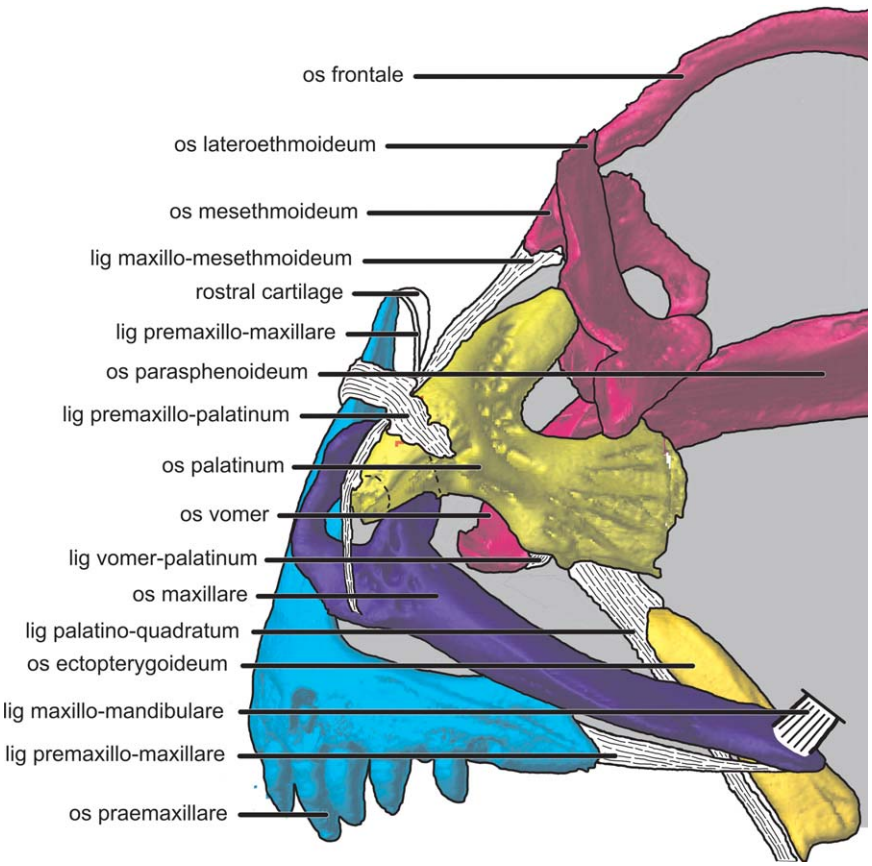

Fig. 5. *P. barbarus*, lateral view on the upper jaw system. The lacrimal bone is not shown. The maxillo-mesethmoideum ligament runs beneath the premaxillo-palatine ligament and connects to the maxillare.

ligamentous connection to the premaxilla on its ventral side (Fig. 5). Anteriorly, at the level of the palatine and premaxilla, the maxilla articulates via a saddle-like process, which forms a complex three-dimensional loop (Figs. 4 and 5). The anterodorsal loop of the maxilla extends medially, posteroventrally of the ascending process of the premaxilla (Fig. 4). This looping process continues as it turns posteroventrally and then laterally to reconnect with the maxilla posterior of its origin. The maxillary loop articulates with the palatine and the ascending arm of the premaxilla. Immediately posterior of this articulation, the maxilla has a secondary process posterior to the palatine. Thus, the anteroventral part of the palatine is surrounded by the processes of the maxilla anteriorly and posteriorly (Figs. 4 and 5). The maxilla is connected to the mesethmoid by a ligament, which runs over the dorsoanterior side of the palatine. The adductor mandibulae A1α muscle connects to the lateral-most side of the dorsal face of the posterior maxilla (Fig. 2B). The premaxilla is V-shaped, with a dorsally directed ascending arm and a dentigerous tooth-bearing arm that runs posteriorly. The premaxilla is held between the anterior processes of the maxillae by the premaxillo-palatine ligament, which runs from the palatine and connects to the anterior face of the ascending arm. The rostral cartilage, which is located posterior to the ascending process, probably protects the ascending process of the premaxilla during mechanical interactions with the premaxilla and maxillar loop. No muscles connect directly to the premaxilla.

Lower jaw. The dentary represents the main structure of the lower jaw and bears several teeth up to the base of the coronoid process (Figs. 2, 3, and 4). The adductor mandibulae A2 muscle connect directly to the posterior and medial side of this process (Fig. 2b). The anguloarticular bone lies immediately medioposteriorly to the ascending process of the dentary, where the retroarticular bone is the most ventral part of the lower jaw. On the medial side of the dentary, the anguloarticular bone is connected by fibrous tissue, which is arranged in various fiber orientations to form a V-shaped pattern (Fig. 6A). The anterior part of the anguloarticular bone inserts partially into a tubular cavity within the medial side of the dentary (Fig. 6B). The Meckelian cartilage runs from the articular part along the length of the bone complex into the tubular cavity to connect within the

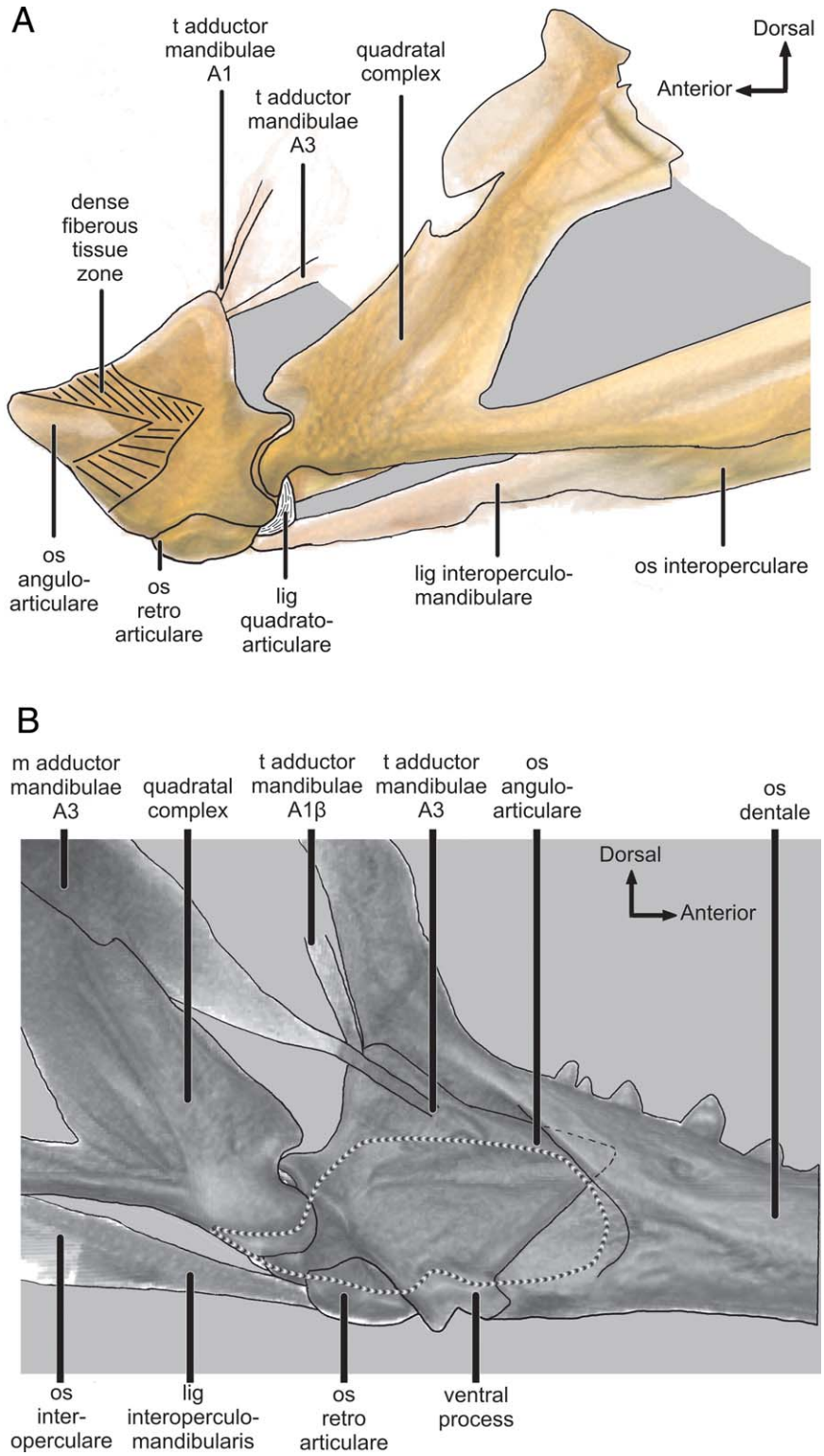

Fig. 6. (**A**) *P. barbarus*, lateral view on the left anguloarticular bone and quadratal complex shown with ligamentous and tendonous connections in volumetric representation of a CT-reconstruction. The area indicated on the anguloarticular bone is where fibrous tissue connects to the medial side of the dentary. The more opaque coloration represents denser material. (**B**) *P. barbarus*, medial view on the joint between lower jaw and quadrate, with tendonous and ligamentous connections. The dotted line represents the area covered by the m. adductor mandibulae Aω.

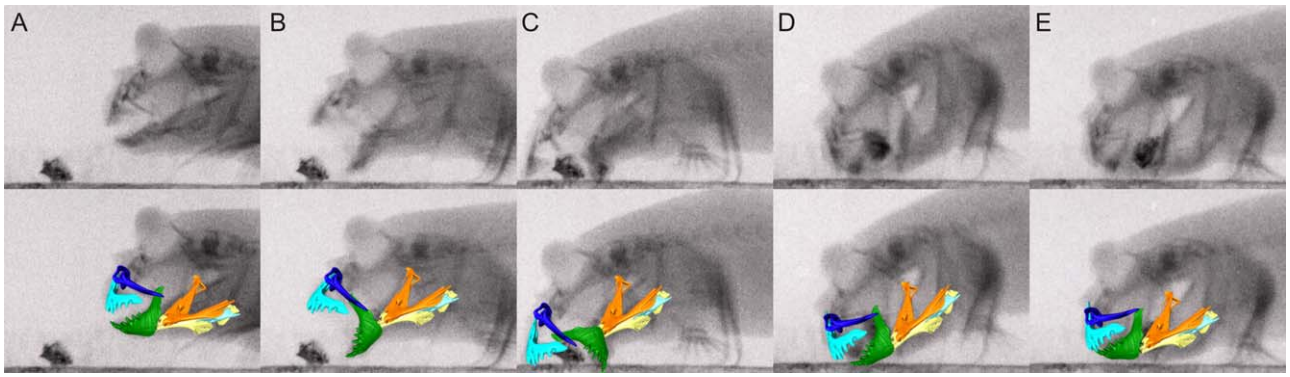

Fig. 7. *P. barbarus*, X-ray images of a typical terrestrial feeding event recorded at 60 fps. Each frame illustrates a representative stage within the feeding event: (**A**) initiation of the prey capture sequence. (**B**) Rotation of the jaws while pivoting the neurocranium and approaching the prey. (**C**) Placement of the jaws over the prey and the end of the neurocranial pivoting onto prey. (**D**) Initial closure of the oral jaws. (**E**) Slow closing and beginning of the reset of the jaws toward the resting position. The bottom row illustrates the position of the premaxillare (light blue), maxillare (dark blue), dentale (green), and quadratal complex (orange/yellow) based on the two-dimensional lateral view. The food particle was soaked in a barium-sulfate solution to be visible on x-ray. The bottom row illustrates a schematic overlay of the position of the bones, not accounting for mediolateral movements.

dentary through the mentomeckelian bone. The posterior zone of the anguloarticular bone is a C-shaped, rounded socket, with pronounced edges dorsally and ventrally of the quadratomandibular joint. These edges have the potential to limit the extent of the depression-elevation rotation of the dentary along the left-right axis. The anguloarticular socket is mediolaterally narrowed, which potentially allows some rotation of the quadratomandibular joint along the dorsoventral axis. On the medioventral side of the anguloarticular bone, a ventral process extends medially immediately anterior to the retroarticular bone. The anguloarticular bone serves as the point of insertion for the tendons of the adductor mandibulae A1β and A3 muscles. The A3 tendon connects onto the coronomeckelian ridge, immediately above the point where the meckelian cartilage enters the anguloarticular bone. The tendon attaches to the ascending process on the medial side of the anguloarticular bone (Fig. 6B). The adductor mandibulae Aω muscle covers most of the medial side of the anguloarticular bone and attaches to the dentary, anguloarticular, and medial side of the quadrate through a small tendon. The interopercular-mandibular ligament attaches to the ventroposterior region of the retroarticular.

Kinematics

Our descriptions of the kinematics focus mainly on the function of the oral jaws, but the movement and timing of other mechanical units are often relevant to the function of the feeding apparatus. Thus, we describe the kinematics during a feeding event in chronological order. Prior to feeding, *P. barbarus* propels itself onto land using its pectoral and caudal fins. In a terrestrial environment, the most common mode of locomotion is a "crutching" gait, which alternates between lifting the body with the pectoral fins and resting on the pelvic fins (Pace and Gibb, 2009; Kawano and Blob, 2013). In our study, *P. barbarus* approached the prey slowly until it was within striking distance (~7–13 cm in our experimental setup). After positioning the pectoral fins anteriorly on either side of the body, the fish propelled itself forward rapidly and the prey capture sequence was initiated. The fish positioned and depressed its head toward and over the prey by pivoting on its pectoral fins. This involved an anteroventral rotation of the neurocranium relative to the earth frame of reference (Fig. 8H). In the following analyses, the positions and angles are expressed relative to the neurocranium, and the rotations are described as clockwise and counterclockwise relative to the animal facing left (as shown in Figs. 1 and 7). The analysis of variance determined no significant differences between individual animals with respect to any of the kinematic variables during prey capture on land ($df = 3$; $F \leq 1.66$; $P \geq 0.34$).

The lower jaw was the first mechanical unit to move during prey capture. As the subject approached the prey, the lower jaw was depressed slowly and the gill covers were elevated while remaining adducted (Fig. 7A). When the mouth was 1.4 ± 0.1 cm from the prey item, lower jaw depression was accelerated (Figs. 7B and 8G), causing the mouth to reach maximum gape within 62 ± 6 ms (Figs. 7C and 8A,G). At the same time, the premaxilla was elevated via a clockwise rotation to reach a maximum upper jaw angle of $141 \pm 4^\circ$ relative to the neurocranium axis (Figs. 1D, 7C, and 8F). During neurocranial pivoting, the premaxillae protruded anteroventrally (Fig. 7C). When the dentary dentition made contact with the substrate, the premaxilla started to be depressed and rotated counterclockwise, thereby decreasing the angle of the upper jaw

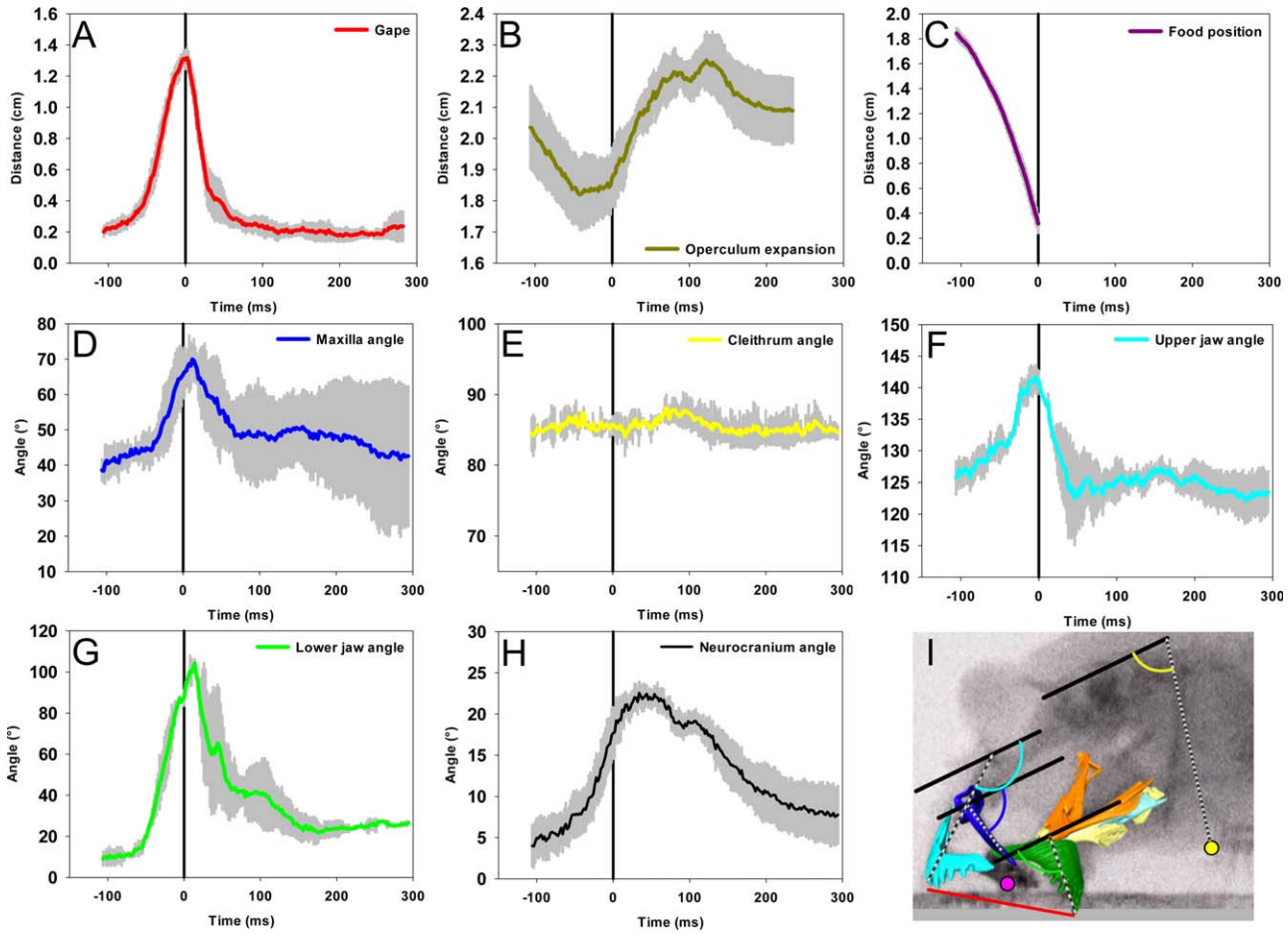

Fig. 8. Graph of the average kinematic variables of *P. barbarus* feeding over time. The color coding corresponds to that of the morphological elements displayed in Fig. 1D. Gape (**A**), Operculum expansion (**B**) and Position to the food relative to the center of the gape (**C**) are displayed in cm. Maxilla angle (**D**), Cleithrum angle (**E**), Upper jaw angle (**F**), Lower jaw angle (**G**), and Neurocranium angle (**H**) are in degree. The gray bars denote the SEM between individuals ($N = 4$). All angles are displayed relative to the Neurocranium angle (H), as measured in Figure 1D. The Neurocranium angle is relative to the earth frame of reference.

relative to the body (Fig. 8F, −6 ms). At this point (Figs. 7C and 8, 0 ms), the maximum gape was reached (maximum gape = 1.29 ± 0.07 cm). Meanwhile, the head continued to move forward and the dentary was depressed further, while the premaxilla angle reduced and the gape size diminished. The dentary then reached its maximum rotation relative to the neurocranium (104 ± 7.8°; Fig. 8G, 18 ms). The maxilla was rotated in the sagittal plane with a slight delay relative to the dentary rotation (Fig. 8D, 15 ± 1.4 ms) and the maxilla did not return to the resting angle at the same time as the lower jaw. The maxilla rotated clockwise in the sagittal plane from around 40° (Fig. 7A) to a maximum of 69 ± 3.7° (Figs. 7C and 8D) relative to the neurocranium after the point of maximum gape (Fig. 8A). As the forward body pivot movement ceased, the lower jaw started to close, thereby reducing the gape rapidly (Figs. 7D and 8G, 36 ± 8.4 ms). When the lower jaw contacted the upper jaw, the upper jaw was retracted and both jaws started to return to their resting position (Fig. 7E).

Based on X-ray recordings, we observed that as the lower jaw closed the hyoid was depressed rapidly, which coincided with a slight abduction of the suspensorium (Fig. 7D). The total counterclockwise rotation of the hyoid was 17.8 ± 1.1°. When the mouth was closed, the hyoid and suspensorium were elevated and adducted, respectively. This was followed by opercular abduction, where the slits in the opercular membranes remained closed until the opercula were fully abducted. After successful prey capture, the opercular membrane slits opened and any excess water and material were expelled. After prey capture, *P. barbarus* generally returned to the water immediately, where the prey likely was processed and swallowed as described by Sponder and Lauder (1981). The overall prey capture sequence, during which the oral jaws opened, the prey was

captured, and the body returned to the resting position, lasted 0.45 ± 0.07 s.

DISCUSSION

The main goal of our study was to identify how the cranial system of *P. barbarus* is morphologically equipped to position its gape above the prey and scoop or grab the prey in its jaws. To achieve this, the mouth opening must be positioned parallel to the substrate while approaching the prey. This implies a considerable reorientation of the mouthparts. Several aspects of the functional morphology of *P. barbarus* play roles in this process and these are discussed later.

The first feature that contributes to a favorable placement of the mouth is the pivoting of the head over the pectoral fins into a nose-down position. As expected, the rotation of the mouth opening because of the pivoting of the neurocranium was limited to about 20° (Fig. 8H). The cleithrum, the main skeletal element that connects the pectoral fins to the neurocranium, was observed to rotate with the neurocranium, the angles between the cleithrum, neurocranium, and vertebral column remained approximately constant during prey capture (Fig. 8E). A firm connection between the cleithrum and the neurocranium was also observed during manipulation of fresh specimens.

Any increase in the angle between the cleithrum and the neurocranium, as typically observed during aquatic suction-feeding (e.g., Van Wassenbergh et al., 2005b; Camp and Brainerd, 2013), would potentially have canceled out the downward tilting of the head by pivoting over the pectoral fins. A rigid pectoral apparatus could be a possible disadvantage for the mudskipper when performing suction feeding as the powerful hypaxial muscles cannot contribute directly to the movement coupled to cleithra retraction, such as mouth opening and hyoid depression. When feeding on land, however, the provision of support and the facilitation of pivoting were the dominant roles of the pectoral apparatus, and not the generation of suction power through retraction of the cleithra.

The lower jaw exhibited an extremely large rotation, which appeared to play an important role in matching the gape to the substrate. Our kinematic data showed that the line connecting the lower jaw tip and the quadratomandibular joint rotated up to $104 \pm 2°$ relative to the neurocranium (Fig. 8G), which is substantial compared to rotation of aquatic and semiaquatic taxa (Labridae: 16 to 42°, Ferry-Graham et al., 2002; Ambystomidea: 33°, Lauder and Shaffer, 1986). The lower jaw was likely rotated by the protractor hyoidei and the hyohyoideus "inferior" muscle, whereby the dentary teeth were oriented perpendicular to the substrate when the gape was placed over the prey item (Fig. 7). On contact with the substrate, the dentary continued to be rotated as the head was moved forward (Fig. 8G). It may be possible for the lower jaw to be passively rotated by the forward movement of the head, thereby forcing the dentary onto the substrate. Manipulations showed that the quadratomandibular joint could only be rotated to approximately 70° relative to the neurocranium. Similarly, based on the morphology of the saddle-like articulation facet of the anguloarticular bone, a maximum rotation of about 70° would be possible before the anguloarticular surface abutted the quadrate socket ventral surface (Fig. 6A,B). These observations suggest that any further rotation would have to derive from movement of the dentary relative to the anguloarticular bone, thereby implying that a considerable amount of intramandibular bending occurs at the level of Meckel's cartilage.

The extensive rotation of the dentary indicates the presence of an intramandibular joint, which has an important role in orienting the mudskipper's gape onto the substrate. Previous studies have identified intramandibular joints with flexion in the sagittal plane in other teleost fish taxa and they are considered to be major functional innovations, which have evolved independently in multiple lineages (Konow et al., 2008). These joints are commonly found in species that feed on items requiring scraping or shearing (Kyphosids, girellids, acanthurids, and chaetodontids; Konow et al., 2008; Ferry-Graham and Konow, 2010), or excavation (pomacanthids; Konow and Bellwood, 2011). These fishes are specialized in mechanically challenging feeding substrata or high force generation. Recent examples have been found in *Girella laevifrons* (Kyphosidae) and *Pomacanthus semicirculatus* (Pomacanthidae), which acquire coral material, hard-shelled invertebrates, or algae via the use of the intramandibular joint (Konow and Bellwood, 2005; Ferry-Graham and Konow, 2010). In *P. barbarus*, the intramandibular joint also facilitates an increased range of motion by the lower jaw. Examinations of histological sections and manipulations of specimens showed that the fibrous connective tissues that connect the lateral side of the anguloarticular bone to the medial side of the dentary allowed considerable freedom of movement (30°). If we combine this with manipulations of the quadratomandibular joint (70°), we explain the measured kinematic angle of the lower jaw during feeding. Based on a combination of the intramandibular joint, quadratomandibular joint, and neurocranium pivot, the dentary may be rotated over a total angle of 120° starting from the resting position. In using an intramandibular joint, the mudskipper shares a mechanism with fishes specialized in the capture of mechanically challenging and partially hidden prey (Konow and Bellwood, 2011), used to capture prey in the terrestrial environment.

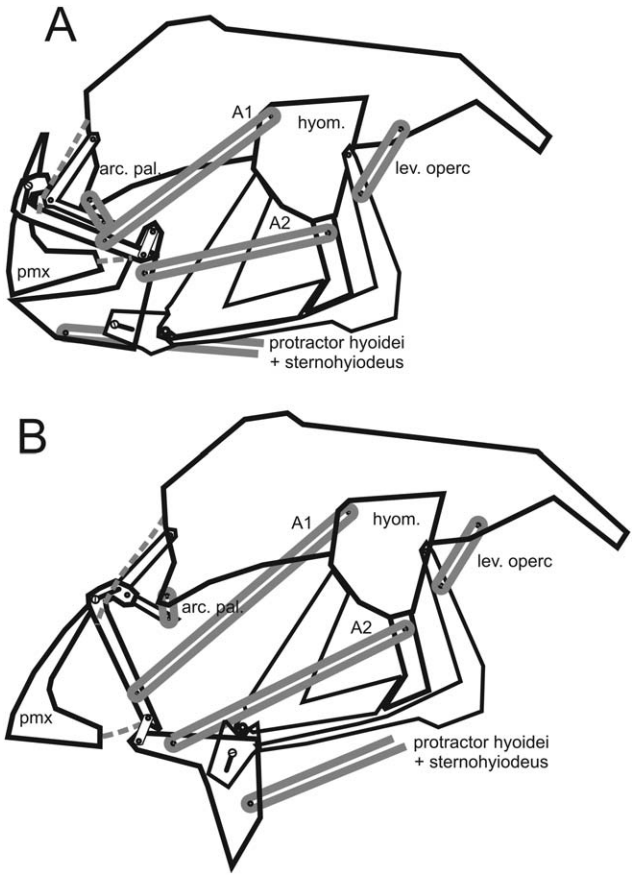

Fig. 9. *P. barbarus*, simplified schematical representation of the main joints, ligaments, and muscles involved in feeding on land. Gray dotted lines represent ligaments, and solid gray lines indicate muscular connections (m. adductor mandibulae A1α and A2, m. adductor arcus palatini, m. levator operculi, m. sternohyoideus, and m. protractor hyoidei). The long axis rotation of the maxillare is not accounted for in this model. The smaller ligamentous insertions of the adductor mandibulae A1β and A3 onto the articular are not take into account in this model.

P. barbarus uses a protrusion mechanism to place the upper jaw on the substrate in front of the prey. In percomorph fishes, the upper jaw elements form a complex mechanism, which allows the upper jaws to move via a complex series of levers and linkages, enabling a number of functions (Eaton, 1935; Randall, 1965; Alexander, 1967; Liem, 1970; Motta, 1984). In *P. barbarus*, similar to most fishes, the protrusion is generated by a coupling with the rotation of the lower jaw: the coronoid process of the dentary moved forward and down, thereby pulling the maxilla with it via the maxillo-mandibular ligament (Figs. 5 and 9B). Via this connection, the dentary rotation pulls the dorsal face of the posterior maxilla medially and down. Both the adductor mandibulae A1α muscle and the maxillo-mesethmoid ligament connect to the lateral side of the maxilla, which creates a rotation along the long axis of the maxilla to an approximate maximum angle of 90° relative to the resting position (Figs. 2B and 4). The longitudinal rotation forces the anterior loop of the maxilla medially and downward in the direction of the midline. The maxillar loop has a thin ligamentous connection with the ascending arm of the premaxilla through the rostral cartilage, where the connection runs posterior of the ascending arm and the rostral cartilage (Figs. 4 and 5). Thus, the maxillar longitudinal rotation "screws" the loop behind the ascending arm of the premaxilla and forces it downward into the protruded position. The premaxilla is physically forced to protrude through the premaxillo-maxillary ligament and the maxillar loop. The relative contributions of these two mechanisms to premaxilla protrusion in the mudskipper cannot be inferred from our data. In *P. barbarus*, a combination of mechanisms of jaw protrusion may be possible. The anterior maxillar loop is very pronounced in the mudskipper (Figs. 4 and 5) relative to that of more generalized aquatic-feeding percomorphs such as *Gasterosteus aculeatus* (Alexander, 1967; Anker, 1974) and *H. elegans* (Otten, 1982), which may indicate a greater role for the maxillar loop in driving the protrusion. Alternatively, the maxillar loop may help to lock the premaxillae into the protruded position via the longitudinal rotation of maxillae. Unfortunately, due to the limited resolution of our high-speed X-ray videos, we were unable to accurately register the longitudinal rotation kinematics of the maxilla. However, we did manage to follow the articulation of the maxilla with the palatine (maxilla angle, Fig. 8D).

In *P. barbarus*, we found that a dorsal rotation of the upper jaw was used to compensate for the ventral pivoting of the head over the pectoral fins. The dorsal rotation of the upper jaw was driven by the depression of the lower jaw. The maxillo-mandibular ligament translated the anterior rotation of the ascending arm of the dentary into a dorsal rotation of the upper jaw (Fig. 8F). As the lower jaw was depressed, the coronoid process of the dentary drove the maxilla forward, thereby translating the maxilla as a whole. The anterior processes of the maxilla then pushed the palatine and premaxilla in the anterior direction. The translation of the whole maxilla was considerable in *P. barbarus* because of the long length of the coronoid process and the dorsal attachment of the maxillo-mandibular ligament compared to overall jaw size. The upper jaw does not articulate directly with the neurocranium, but indirectly through the palatine, which allowed the forward movement of the maxilla to rotate the premaxilla anteriorly and upward by 20° (Figs. 5 and 8F). The palatine articulation was controlled by the anterior subdivision of the adductor arcus palatini muscle and the vomer-palatine ligament (Fig. 3). The 20° dorsal rotation of the premaxilla compensated for the nose-down rotation of the head

(neurocranium rotation, Fig. 8H), which was needed to position the oral jaws straight in front of the prey item. The system of palatine articulation, dorsal rotation of the upper jaw, and protrusion by twisting the maxilla are not unique to mudskippers and has been described in other Perciformes and in Zeiformes (dories; Westneat, 2003). Our study showed that the considerable rotation and articulation of the palatine allows the directing of the "modified nipping type" upper jaws (Gregory, 1933) toward and onto ground-based prey on land.

After gape placement over the prey, the jaws must be closed to capture the prey between the jaws. In *P. barbarus*, mouth closure was achieved almost exclusively by movement of the lower jaw. The mudskipper moved the teeth of the lower jaw closely along the substrate, thereby scooping up the prey item into the oral cavity or capturing the prey between the upper and lower jaws. The upper jaw remained protruded until contact with the lower jaw, after which the mouth closed almost completely and the lower jaw rotation slowed down. The lower jaw continued to rotate, pushing the upper jaw back toward the starting position (Figs. 7E and 8F). In all of the terrestrial feeding events we observed, the upper jaw required direct contact with the lower jaw to retract from the protruded position. This suggests that the upper jaw may only have a passive retraction system. The head was lifted to the horizontal starting position after jaw closure (Fig. 8H).

The angular velocity of lower jaw closure was remarkably high in terrestrial feeding mudskippers. The average closure speed of the lower jaw from start until contact with the upper jaw was $1.3 \pm 0.3 \times 10^{3\circ}\ s^{-1}$, which is higher than that reported for other animals (Ambystomidea: $9.1 \times 10^{2\circ}\ s^{-1}$, Lauder and Shaffer, 1986; Labridae: $361–674^\circ\ s^{-1}$, Ferry-Graham et al., 2002; Clariidea : $1.0–1.2 \times 10^{3\circ}\ s^{-1}$, Van Wassenbergh et al., 2005a). The average time required to close the mouth (36 ms) was comparable to data obtained from similar-sized species (Ambystomidea: 36 ms, Labridae: 21–73 ms, Clariidea: 20–50 ms) but the mudskipper managed to rotate its lower jaw by a much greater angle within this time. How does *P. barbarus* close its lower jaw so rapidly? The following factors might contribute to the velocity of lower jaw closure in the mudskipper: 1) the adductor musculature orientation, their points of connection to skeletal elements, and the subsequent moment arms; 2) the intramandibular joint; and 3) the effect of the terrestrial environment.

Mouth closure is powered mainly by the adductor mandibulae musculature, which means that the properties of the leverage system of these muscles should contribute to the speed of lower jaw closure (Fig. 9). In the mudskipper, the adductor mandibulae A2 is the only muscle directly connected to the dentary and inserts onto the long coronoid process. The length of the coronoid process and the dorsal point of insertion of the A2 may provide a potentially high mechanical advantage during the lower jaw closure (Westneat, 2003; Konow and Bellwood, 2005). However, the length of the coronoid process may have a negative effect on the closing velocity of the lower jaw because of its poor gearing for generating speed. In other words, due to the long coronoid process in-lever moment arm, a given shortening of the adductor mandibulae A2 will result in a relatively small rotation around the quadratomandibular joint (Fig. 9A). However, at the maximum lower jaw depression angle, the effective in-lever moment arm is very small because the muscle has to pass very close to the quadratomandibular joint (Fig. 9B). Thus, at maximum lower jaw depression, even a small shortening of the A2 muscle would result in a relatively large rotation around the quadratomandibular joint. The effective mechanical advantage of the lower jaw closing relative to the adductor mandibulae A2 muscle changes significantly during lower jaw elevation, beginning with a low mechanical advantage but high velocity rotation and ending with a high mechanical advantage but low velocity rotation (Fig. 9). This makes the generation of force to close the mouth increasingly more difficult with an increasing lower jaw depression angle. A sufficiently long lever arm relative to the quadratomandibular joint is needed to make mouth closure possible at increased lower jaw depression angles. Therefore, the relatively long coronoid process of *P. barbarus* may be necessary to allow sufficient force generation even at maximum lower jaw depression (Fig. 9B).

The adductor mandibulae A1 and A3 muscles may also contribute to rapid closure via their respective points of connection relative to the lower jaw. The adductor mandibulae A1α's connection to the lateral side of maxilla allows muscle to be an indirect but effective jaw closer, even at the maximum lower jaw depression (Fig. 9). By adding part of the maxilla to the effective lever arm of the coronoid process, the length of the in-lever moment arm is greater than the lower jaw out-lever relative to the quadratomandibular joint (Fig. 9B). The position and direction from which the adductor mandibulae A1α can act on the lower jaw through the maxilla provides a high mechanical advantage (Fig. 9B). The combination of the adductor mandibulae A1α and A2 lever moment arms may facilitate both a fast and forceful lower jaw elevation. In addition, the tendonous connection of the A1β on the ascending process of the anguloarticular is in close proximity to the quadratomandibular joint (Fig. 6). During lower jaw closure, both the adductor mandibulae A3 and the A1β division of the A1 helps the return of the lower jaw to the resting position through the anguloarticular bone. The lever arm

attributed to these tendinous insertions is small and the tendons pass very close to the quadratomandibular joint at maximum lower jaw depression. This makes the A3 and A1β effective only at a low mechanical advantage but with a high velocity contribution to the jaw closure.

The elastic energy stored by rotating the intramandibular joint could contribute to the rapid closure of the lower jaw. Manipulation of the intramandibular joint using fresh material detected a resistance to bending and a return to the resting orientation of the anguloarticular bone relative to the dentary. The freedom of movement of the intramandibular joint is attributable to Meckel's cartilage and the connective tissue, which may allow the storage of elastic energy (potentially similar to that described by Aerts, 1985). The kinematic data for the lower jaw did not allow us to determine whether the intramandibular joint is actively retracted or elastically closed, due to contact of the lower jaw with the substrate. The joint may, therefore, also serve as a method of reducing the risk of injury as the lower jaw bends on impact with the ground during downward movement of the head.

Finally, the relatively low fluid dynamic resistance of the air in the terrestrial environment compared with the aquatic environment may have a positive effect on the lower jaw closure speed of *P. barbarus*. Structures may move more rapidly on land because the force required to overcome the inertia of air surrounding the lower jaw is less than water due to the difference in density. Thus, differences in the fluid dynamics involved could facilitate more rapid feeding movements on land. Theoretically, each of these factors could contribute to the high rotational velocity of lower jaw closure in *P. barbarus*, but the current data did not allow us to determine the specific contributions of these factors to the total rotation of the lower jaw.

In conclusion, we found that *P. barbarus* was capable of reorienting its mouth aperture to allow it to scoop prey from the ground using its oral jaws via a combination of factors. First, pivoting the neurocranium over the pectoral appendages rotated the jaws ventrally. Second, the complex upper-jaw linkage system allowed the premaxilla to protrude and rotate dorsally. Finally, the dentary part of the lower jaw exhibited an impressive posterior rotation, which was facilitated by the action of an intramandibular joint. The rapid mouth closure movement of the dentary allowed the prey to be grabbed between the upper and lower jaws, or scooped into the mouth. The high closure speed of the dentary was probably related to the line of action of the adductor mandibulae A2, which is geared for speed at high gape angles, while it may also have been assisted by the elastic recoil of the intramandibular bending. These results highlight the importance of the specific positioning of the jaws during the capture of ground-based prey, which was demonstrated previously in eel catfish (Van Wassenbergh, 2013). However, these two groups (mudskippers and eel catfish) have remarkably different cranial morphologies and feeding kinematics, thus more than one combination of fish bauplan and behavior appears to allow the efficient terrestrial capture of prey.

ACKNOWLEDGMENT

We would like to thank two anonymous reviewers and Nicolai Konow for their helpful comments and insight.

Author Contributions: P.A. and S.V.W. conceived the study; S.V.W. and K.M. preformed the video recordings; D.A. provided technical support; E.D. preformed the CT-scan; K.M. collected and analysed the data, and wrote the manuscript; S.V.W, P.A. and D.A. helped with data interpretation and writing of the manuscript.

LITERATURE CITED

Aerts P. 1985. The Intramandibular Linkage in *Astatotilapia elegans* (Teleostei, Cichlidae)–appearance and function of the meckelian cartilage. J Zool 205:391–410.

Ahlberg PE, Clack JA, Luksevics E, Blom H, Zupins I. 2008. *Ventastega curonica* and the origin of tetrapod morphology. Nature 453(7199):1199–1204.

Alexander R. 1967. The functions and mechanisms of the protrusible upper jaws of some acanthopterygian fish. J Zool 151(1):43–64.

Anker G. 1974. Morphology and kinetics of the head of the stickleback, *Gasterosteus aculeatus*. Trans Zool Soc London 32(5):311–416.

Anker GC. 1977. The morphology of the head-muscles of a generalized *Haplochromis* species: *H. elegans* Trewavas 1933 (Pisces, Cichlidae). Neth J Zool 28(2):234–271.

Anker GC. 1985. The morphology of joints and ligaments in the head of a generalized *Haplochromis* species: *H. elegans* Trewavas 1933 (Teleostei, Cichlidae). Neth J Zool 36(4):498–529.

Arratia, G. 1987. Description of the primitive family Diplomystidae (Siluriformes, Teleostei, Pisces): Morphology, taxonomy and phylogenetic implications. Bonn Zool Monogr 24:1–120.

Ashley-Ross MA, Hsieh ST, Gibb AC, Blob RW. 2013. Vertebrate land invasions-past, present, and future: An introduction to the symposium. Integr Comp Biol 53(2):192–196.

Barel C, Witte F, van Oijen M. 1976. The shape of the skeletal elements in the head of a generalized *Haplochromis* species: *H. elegans* Trewavas 1933 (Pisces, Cichlidae). Neth J Zool 26:163–265.

Boisvert CA. 2005. The pelvic fin and girdle of *Panderichthys* and the origin of tetrapod locomotion. Nature 438(7071): 1145–1147.

Bradford Y, Conlin T, Dunn N, Fashena D, Frazer K, Howe DG, Knight J, Mani P, Martin R, Moxon SA, Paddock H, Pich C, Ramachandran S, Ruef BJ, Ruzicka L, Bauer Schaper H, Schaper K, Shao X, Singer A, Sprague J, Sprunger B, Van Slyke C, Westerfield M. 2011 ZFIN: Enhancements and updates to the zebrafish model organism database. Nucleic Acids Res 39(suppl 1):D822–D829.

Burgess W, Axelrod HR, Hunziker RE. 1990. Atlas of marine aquarium fishes. THF Publications.

Camp AL, Brainerd EL. 2014. Role of axial muscles in powering mouth expansion during suction feeding in Largemouth Bass. J Exp Biol 217(8):1333–1345.

Daeschler EB, Shubin NH, Jenkins FA Jr. 2006. A Devonian tetrapod-like fish and the evolution of the tetrapod body plan. Nature 440(7085):757–763.

Downs JP, Daeschler EB, Jenkins FA Jr, Shubin NH. 2008. The cranial endoskeleton of *Tiktaalik roseae*. Nature 455(7215): 925–929.
Eaton TH. 1935. Evolution of the upper jaw mechanism in teleost fishes. J Morphol 58(1):157–172.
Elshoud-Oldenhave MJ. 1979. Prey capture in the pike-perch, *Stizostedion lucioperca* (Teleostei, Percidae): A structural and functional analysis. Zoomorphology 93(1):1–32.
Erer KS. 2007. Adaptive usage of the Butterworth digital filter. J Biomech 40(13):2934–2943.
Ferry-Graham LA, Konow N. 2010. The intramandibular joint in *Girella*: A mechanism for increased force production? J Morphol 271(3):271–279.
Ferry-Graham LA, Wainwright PC, Westneat MW, Bellwood DR. 2002. Mechanisms of benthic prey capture in wrasses (Labridae). Mar Biol 141(5):819–830.
Gans C. 1969. Functional components versus mechanical units in descriptive morphology. J Morphol 128(3):365–383.
Geerinckx T, Herrel A, Adriaens D. 2011. Suckermouth armored catfish resolve the paradox of simultaneous respiration and suction attachment: A kinematic study of *Pterygoplichthys disjunctivus*. J Exp Zool A Ecol Genet Physiol 315(3):121–131.
Gibb AC, Ashley-Ross MA, Pace CM, Long JH Jr. 2011. Fish out of water: Terrestrial jumping by fully aquatic fishes. J Exp Zool A Ecol Genet Physiol 315(10):649–653.
Gillis GB. 1998. Environmental effects on undulatory locomotion in the American eel *Anguilla rostrata*: Kinematics in water and on land. J Exp Biol 201(7):949–961.
Gordon MS, Boëtius I, Evans DH, McCarthy R, Oglesby LC. 1969. Aspects of the physiology of terrestrial life in amphibious fishes I. The mudskipper, *Periophthalmus sobrinus*. J Exp Biol 50(1):141–149.
Gregory WK. 1933. Fish skulls: A study of the evolution of natural mechanisms. Trans Am Phil Soc (NS) 23:481 p.
Harrington RW. 1955. The osteocranium of the American cyprinid fish, *Notropis bifrenatus*, with an annotated synonymy of teleost skull bones. Copeia 1955(4):267–290.
Harris VA. 1960. On the locomotion of the mudskipper Periophthalmus koelreuteri (pallas): (gobiidae). Proceedings of the Zoological Society of London 134:107–135.
Herrel A, Van Wassenbergh S, Aerts P. 2012. Biomechanical studies of food and diet selection. eLS. Available at: http://onlinelibrary.wiley.com/doi/10.1002/9780470015902.a0003213.pub2/full.
Hsieh S-TT. 2010. A locomotor innovation enables water-land transition in a marine fish. PloS one 5(6):e11197.
Kawano SM, Blob RW. 2013. Propulsive forces of mudskipper fins and salamander limbs during terrestrial locomotion: Implications for the invasion of land. Integr Comp Biol 53(2): 283–294.
Konow N, Bellwood DR. 2005. Prey-capture in *Pomacanthus semicirculatus* (Teleostei, Pomacanthidae): Functional implications of intramandibular joints in marine angelfishes. J Exp Biol 208(8):1421–1433.
Konow N, Bellwood DR. 2011. Evolution of high trophic diversity based on limited functional disparity in the feeding apparatus of marine angelfishes (f. Pomacanthidae). PloS one 6(9):e24113.
Konow N, Bellwood DR, Wainwright PC, Kerr AM. 2008. Evolution of novel jaw joints promote trophic diversity in coral reef fishes. Biol J Linn Soc 93(3):545–555.
Lauder G. 1985. Aquatic feeding in lower vertebrates. In: Hildebrand DMBM, Liem KF, Wake D, editors. Functional Vertebrate Morphology. Cambridge, Massachusetts: Harvard Univ. Press. p 210–229.
Lauder GV, Shaffer HB. 1986. Functional design of the feeding mechanism in lower-vertebrates–unidirectional and bidirectional flow systems in the tiger salamander. Zool J Linn Soc 88(3):277–290.
Liem KF. 1970. Comparative functional anatomy of the Nandidae (Pisces: Teleostei). Chicago: Field Museum of Natural History.
Liem KF. 1990. Aquatic versus terrestrial feeding modes: Possible impacts on the trophic ecology of vertebrates. Am Zool 30(1):209–221.
Masschaele BC, Cnudde V, Dierick M, Jacobs P, Van Hoorebeke L, Vlassenbroeck J. 2007. UGCT: New x-ray radiography and tomography facility. Nucl Instrum Methods Phys Res A 580(1):266–269.
Motta PJ. 1984 Mechanics and functions of jaw protrusion in teleost fishes: A review. Copeia 1984(1):1–18.
Nieder J. 2001. Amphibious behaviour and feeding ecology of the four-eyed blenny (*Dialommus fuscus*, Labrisomidae) in the intertidal zone of the island of Santa Cruz (Galapagos, Ecuador). J Fish Biol 58(3):755–767.
Nowroozi BN, Brainerd EL. 2014. Importance of mechanics and kinematics in determining the stiffness contribution of the vertebral column during body-caudal-fin swimming in fishes. Zoology (Jena) 117:28–35.
Otten E. 1982. The jaw mechanism during growth of a generalized *Haplochromis* species: *H. elegans* Trewavas 1933 (Pisces, Cichlidae). Neth J Zool 33(1):55–98.
Pace CM, Gibb AC. 2009. Mudskipper pectoral fin kinematics in aquatic and terrestrial environments. J Exp Biol 212(14): 2279–2286.
Pierce SE, Hutchinson JR, Clack JA. 2013. Historical perspectives on the evolution of tetrapodomorph movement. Integr Comp Biol 53(2):209–223.
Randall JE. 1965. Grazing effect on sea grasses by herbivorous reef fishes in the West Indies. Ecology 46(3):255–260.
Sayer M, Davenport J. 1991. Amphibious fish: Why do they leave water? Rev Fish Biol Fish 1(2):159–181.
Schoenfuss HL, Blob RW. 2003. Kinematics of waterfall climbing in Hawaiian freshwater fishes (Gobiidae): Vertical propulsion at the aquatic–terrestrial interface. J Zool 261(2):191–205.
Shubin NH, Daeschler EB, Jenkins FA Jr. 2006. The pectoral fin of *Tiktaalik roseae* and the origin of the tetrapod limb. Nature 440(7085):764–771.
Snelderwaard P, De Groot JH, Deban SM. 2002. Digital video combined with conventional radiography creates an excellent high-speed X-ray video system. J Biomech 35(7):1007–1009.
Sponder DL, Lauder GV. 1981. Terrestrial feeding in the mudskipper *Periophthalmus* (Pisces, teleostei)–a Cineradiographic analysis. J Zool 193:517–530.
Stebbins RC, Kalk M. 1961. Observations on the natural history of the mud-skipper, *Periophthalmus sobrinus*. Copeia 1961(1):18–27.
Summers AP, Darouian KF, Richmond AM, Brainerd EL. 1998. Kinematics of aquatic and terrestrial prey capture in *Terrapene carolina*, with implications for the evolution of feeding in cryptodire turtles. J Exp Zool 281(4):280–287.
Van Wassenbergh S. 2013. Kinematics of terrestrial capture of prey by the eel-catfish *Channallabes apus*. Integr Comp Biol 53(2):258–268.
Van Wassenbergh S, Aerts P, Adriaens D, Herrel A. 2005a. A dynamic model of mouth closing movements in clariid catfishes: The role of enlarged jaw adductors. J Theor Biol 234(1):49–65.
Van Wassenbergh S, Herrel A, Adriaens D, Aerts P. 2005b. A test of mouth-opening and hyoid-depression mechanisms during prey capture in a catfish using high-speed cineradiography. J Exp Biol 208(24):4627–4639.
Van Wassenbergh S, Herrel A, Adriaens D, Huysentruyt F, Devaere S, Aerts P. 2006. Evolution: A catfish that can strike its prey on land. Nature 440(7086):881.
Vlassenbroeck J, Dierick M, Masschaele B, Cnudde V, Van Hoorebeke L, Jacobs P. 2007. Software tools for quantification of X-ray microtomography at the UGCT. Nucl Instrum Methods Phys Res A 580(1):442–445.
Westneat MW. 2003. A biomechanical model for analysis of muscle force, power output and lower jaw motion in fishes. J Theor Biol 223(3):269–281.
Winter, D.A. (2004) Biomechanics and Motor Control of Human Movement. New York: Wiley.
Winterbottom R. 1973. A descriptive synonymy of the striated muscles of the Teleostei. Proc Acad Natl Sci Philadelphia: 225–317.